PALEONTOLOGY

The extinct shark *Otodus megalodon* was a transoceanic superpredator: Inferences from 3D modeling

Jack A. Cooper[1], John R. Hutchinson[2]*, David C. Bernvi[3], Geremy Cliff[3,4], Rory P. Wilson[1], Matt L. Dicken[3,5], Jan Menzel[6], Stephen Wroe[7], Jeanette Pirlo[8,9], Catalina Pimiento[1,10,11]*

Although shark teeth are abundant in the fossil record, their bodies are rarely preserved. Thus, our understanding of the anatomy of the extinct *Otodus megalodon* remains rudimentary. We used an exceptionally well-preserved fossil to create the first three-dimensional model of the body of this giant shark and used it to infer its movement and feeding ecology. We estimate that an adult *O. megalodon* could cruise at faster absolute speeds than any shark species today and fully consume prey the size of modern apex predators. A dietary preference for large prey potentially enabled *O. megalodon* to minimize competition and provided a constant source of energy to fuel prolonged migrations without further feeding. Together, our results suggest that *O. megalodon* played an important ecological role as a transoceanic superpredator. Hence, its extinction likely had large impacts on global nutrient transfer and trophic food webs.

INTRODUCTION

Computer modeling has given paleontologists the unprecedented ability to use exceptionally well-preserved fossils to reconstruct the entire body of extinct animals, which in turn allows estimations of biological traits from the resulting geometry (*1–4*). For example, complete skeletons of *Tyrannosaurus rex* have been used to estimate an adult mass of ~5000 to 10,000 kg (*1, 3, 4*). This task is, however, considerably harder for extinct sharks, whose cartilaginous skeletons have poor preservation potential in the fossil record and usually only leave behind teeth and occasionally vertebrae (*5*). Therefore, biological traits of extinct sharks are typically inferred on the basis of extrapolations from close relatives and ecological analogs.

Otodus megalodon, a member of the extinct family Otodontidae (order: Lamniformes), was the largest known macropredatory shark (*6*). Fossil remains of this extinct giant consist mainly of teeth. On the basis of the age, morphology, and worldwide distribution of these teeth, it has been proposed that this species was a cosmopolitan predator that lived from the Miocene to the Pliocene [23 to 2.6 million years (Ma) ago; (*6–10*)]. Its extinction has been attributed to a reduction of productive coastal habitats in the late Pliocene, which likely caused the loss of other marine megafaunal species, many of which could have been *O. megalodon* prey, and the appearance of potential competitors (*9, 11*).

The body length of the iconic *O. megalodon* has been inferred on the basis of tooth measurements and comparisons with the extant great white shark (*Carcharodon carcharias*: order Lamniformes, family Lamnidae), which is regarded as the best available ecological analog despite belonging to a different family (*12, 13*). For instance, extrapolations of the relationship between tooth crown height and total length (i.e., length from the snout to the tip of the tail; herein TL) in *C. carcharias* (*12*) have suggested a maximum TL of 14 to 18 m for *O. megalodon* (*6, 7, 13*). More recently, however, a maximum TL of 20 m has been calculated on the basis of the tooth crown width of associated dentitions of other lamniform sharks (*14*). The dimensions of *O. megalodon* body parts have also been estimated using multiple lamniform analogs, suggesting that an adult ~16-m *O. megalodon* would have had a head 4.7 m long, a dorsal fin 1.6 m tall, and a tail about 4 m high (*15*).

The body mass of *O. megalodon* at different life stages (e.g., ~48,000 kg for a ~16-m individual) has also been estimated on the basis of vertebral centra and extrapolations from *C. carcharias* (*7*). Vertebral columns hardly ever preserve, with only two specimens to our knowledge reported from Miocene deposits of Belgium and Denmark (*7, 16*). The column from Belgium consists of 141 centra (IRSNB P 9893; formerly labeled IRSNB 3121) and was previously examined by Gottfried *et al.* (*7*), who concluded that it belonged to a single individual, undoubtedly an exceptional fossil due to the sheer number of centra preserved. Although a recent study examined the growth bands of three of the centra and concluded that IRSNB P 9893 died at age 46 (*17*), no study, prior or since, has attempted to reconstruct this specimen in detail based on its vertebral column.

Fossil evidence of bite marks on bones has shed some light on the autoecology of *O. megalodon* (*18–21*). For instance, it has been hypothesized that *O. megalodon* preferentially preyed on small- to medium-size cetaceans [e.g., 2.5 to 7 m; (*19, 20*)] such as the extinct *Piscobalaena nana* (*19*) and *Xiphiacetus bossi* (*20*). Larger prey includes taxa related to the modern humpback (*Megaptera novaeangliae*) or blue whales [*Balaenoptera musculus*; (*18*)]. Evidence from calcium isotopes has further suggested that *O. megalodon* occupied a higher trophic level than did *C. carcharias* (*22*), which typically consumes comparatively small prey in their entirety [e.g., sharks, *Carcharhinus obscurus* and *Prionace glauca*, and dolphins, *Tursiops truncatus* and *Delphinus delphis*; (*23, 24*)], and travels great distances across oceans (*25*). Last, it has been proposed that an adult *O. megalodon* could

[1]Department of Biosciences, Swansea University, Swansea SA2 8PP, UK. [2]Structure and Motion Laboratory, Department of Comparative Biomedical Sciences, Royal Veterinary College, Hawkshead Lane, Hatfield, Hertfordshire AL9 7TA, UK. [3]KwaZulu-Natal Sharks Board, Umhlanga Rocks 4320, South Africa. [4]School of Life Sciences, University of KwaZulu-Natal, Durban, KZN, South Africa. [5]School of Biological and Marine Sciences, University of Plymouth, Plymouth, PL4 8AA, UK. [6]JanMenzelArt, Stellenbosch 7600, South Africa. [7]Function, Evolution, and Anatomy Research Lab, School of Environmental and Rural Science, University of New England, Armidale, NSW 2351, Australia. [8]Department of Biology, University of Florida, Gainesville, FL 32611, USA. [9]Department of Biological Sciences, California State University Stanislaus, Turlock, CA 95382, USA. [10]Paleontological Institute and Museum, University of Zurich, Zurich CH-8006, Switzerland. [11]Smithsonian Tropical Research Institution, Balboa, Panama.
*Corresponding author. Email: catalina.pimientohernandez@pim.uzh.ch (C.P.); jhutchinson@rvc.ac.uk (J.R.H.)

reach cruising speeds of 1.3 to 1.4 m/s (*26*, *27*) and burst speeds of 10.3 m/s (*26*), and that such an ability was enhanced by mesothermy (*26*), a thermoregulatory adaptation that elevates the temperature of locomotory muscles (*28*). The purported mesothermic physiology of *O. megalodon* has been supported by multiple lines of evidence, including comparative analyses, stable isotopes, and species distribution models (*9*, *26*, *29*).

Notwithstanding these advances in the understanding of *O. megalodon*, its full-body anatomy and critical aspects of its ecology remain unclear or outdated. For instance, its body mass, a key trait to infer other ecophysiological properties, was last estimated in the early 1990s based on the assumption that *C. carcharias* is a direct descendant of *O. megalodon* (*7*), which has since been disfavored (*30*). Given the most recent advances in computer modeling, it is now possible to make a more comprehensive and up-to-date reconstruction of *O. megalodon* to estimate various biological traits of this extinct shark.

Here, we create the first three-dimensional (3D) model of the body of *O. megalodon* and use it to infer its movement and feeding ecology. We first reconstructed the axial skeleton using 3D scans of the exceptional vertebral column IRSNB P 9893 from Belgium, an associated dentition from the United States, and a *C. carcharias* chondrocranium (Fig. 1 and figs. S1 and S2). We completed the model by adding "flesh" around the skeleton using a full-body scan of *C. carcharias* (Fig. 1) and adjusted it based on a 2D reconstruction of *O. megalodon* that accounts for other analogs [i.e., *Isurus* and *Lamna* spp.; see Materials and Methods; (*15*)]. We quantified TL, volume, and gape size from the complete 3D model. Volume was then used to calculate body mass. Last, we estimated the model's swimming speed, stomach volume, daily energetic demands, and prey encounter rates based on their mathematical relationships with mass in extant sharks. Our results reveal the potentially distinctive ecological role that *O. megalodon* played in the global oceans, advancing our knowledge of the impacts of megafaunal species on marine ecosystems in deep time and the potential ecological consequences of their extinctions.

RESULTS
Anatomical reconstruction
We used a hoop-based approach to build a 3D model of the full body of *O. megalodon* in Blender 2.80 (www.blender.org). We adjusted the initial model based on a previous 2D reconstruction (*15*) to account for phylogenetic uncertainties and the intraspecific variation among lamniforms (see Materials and Methods). The complete model (Fig. 1) was first measured directly in Blender, rendering a TL of 15.9 m (Table 1). Then, it was imported into MeshLab (*31*), where a volume of 58.1 m^3 was computed. We used this volume and its relationship with the density of pelagic sharks relative to seawater (*32*) to calculate a body mass of 61,560 kg (Table 1). Although our methodology (*1–4*) is considered to provide precise mass estimates in extant and extinct taxa (*2*, *3*), we tested its best-case validity based on a *C. carcharias* specimen of known size. To do so, we measured the volume of our *C. carcharias* full-body scan (Fig. 1G; see Materials and Methods), estimated its mass, and compared it with the mass empirically measured (164 kg; see Materials and Methods). We found the mass estimated from the volumetric 3D scan to be 17.5% lower than that the mass reported from the specimen when it was weighed in situ.

Swimming speed estimations
We calculated the absolute cruising speed (meters per second, herein in m/s) of the modeled *O. megalodon* using a previously established relationship between speed and body mass, based on 391 individuals across 28 extant shark species (*33*). We also converted this calculation to relative cruising speed (body lengths per second, herein BL/s). Our results suggest a mean absolute speed of 1.4 m/s (5 km/hour), with a 95% confidence interval (CI) of 0.5 to 4.1 m/s. Mean relative cruising speed was 0.09 BL/s (95% CI = 0.03 to 0.26 BL/s; Table 1). The wide CI values of these calculations reflect the size variation in extant sharks and the inherent uncertainties of estimating biological properties for extinct animals, especially one of such enormous size compared to its living relatives. Considering that the upper CIs are particularly implausible for such a large shark (*34*), our inferences and interpretations are based on the mean cruising speed, which, although not assumed to be accurate, agrees with previous estimates (*26*, *27*).

We contrasted the estimated mean absolute cruising speed of the model against the mean values of the 28 species mentioned above [see Materials and Methods; (*33*)] and found that a ~16-m *O. megalodon* was able to cruise faster than all living species considered (data S1), including the mesothermic salmon shark (*Lamna ditropis*), porbeagle shark (*Lamna nasus*), and great white shark (*C. carcharias*; Fig. 2A). We also compared the mean absolute cruising speed of the model with the 391 individuals belonging to the 28 species and found that a ~16-m *O. megalodon* (Fig. 2B, #1) could swim 7 times faster than the largest individual in the dataset, an 18-m TL, 24,800-kg whale shark (*Rhincodon typus*, an ectothermic filter feeder; Fig. 2B, #2), and 60 times faster than the slowest individual, a 4-m TL, 215-kg *R. typus* (Fig. 2B, #3). Conversely, the model's estimated absolute cruising speed was two times slower than that of four mesothermic macropredators: three *C. carcharias* of 428, 874, and 750 kg (3.6, 4.6, and 4.4-m TL; Fig. 2B, #4, #5, and #6, respectively) and a 16-kg (1.1-m TL) *Isurus oxyrinchus* (Fig. 2B, #7). Furthermore, the absolute cruising speed of the model was similar to that of a 3800-kg (8-m TL) *Cetorhinus maximus* (an ectothermic filter feeder; Fig. 2B, #8), a 494-kg (3.8-m TL) *C. carcharias* (Fig. 2B, #9), and a 23-kg (1.42-m TL) *I. oxyrinchus* (Fig. 2B, #10). We repeated these comparisons using relative cruising speed, which is adjusted to body size (see Materials and Methods). As expected, given the nature of the metric, at 0.09 BL/s, the ~16-m *O. megalodon* model was found to be slower than almost all macropredatory sharks (fig. S3A) but remained considerably faster than filter feeders of similar size (i.e., an 18-m *R. typus* swimming at 0.01 BL/s; fig. S3B, #2).

Prey intake estimations
We estimated the model's gape size and stomach volume to infer maximum prey size. Gape size was quantified in Blender at different angles (fig. S4). Our calculations indicated a gape height of 1.2 m at a 35° angle and of 1.8 m at 75°. Gape width measured 1.7 m at both 35° and 75° angles (Table 1). To estimate stomach volume, we determined the relationship between body mass and stomach volume in *C. carcharias* by dissecting and examining the stomachs of 12 individuals (see Materials and Methods). We used *C. carcharias* as the sole proxy for this and subsequent prey intake analyses because of their inferred similarities in diet and metabolism (*19*, *20*, *26*, *35*). Our results suggest that the model *O. megalodon* had a stomach of 9605 liters (95% CI = 8487 to 10,722 liters; Table 1). We compared our results against the size of potential contemporaneous prey as
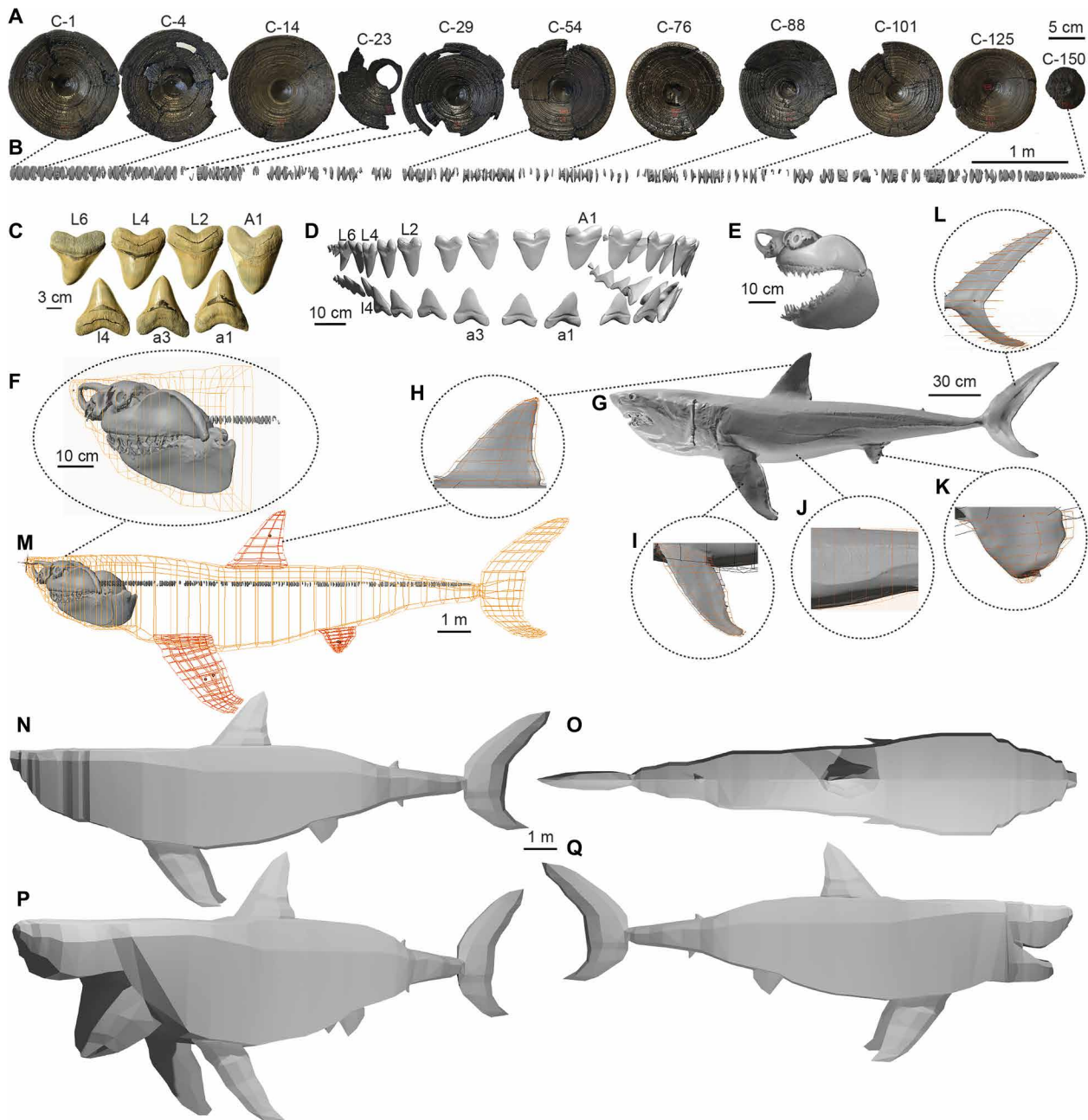
Fig. 1. Modeling procedure. (**A**) Sample of 11 of the 141 vertebral centra in the *Otodus megalodon* column (IRSNB P 9893). (**B**) 3D scan and reconstruction of the *O. megalodon* vertebral column, with centra from (A) linked to their corresponding position. (**C**) Sample of seven *O. megalodon* teeth from the UF 311000 dentition (lingual view) with their respective positions (uppercase denotes upper teeth; lowercase refers to lower teeth; "A" denotes anterior teeth, and "L" lateral). (**D**) 3D scan and reconstruction of the UF 311000 dentition (labial view) with the corresponding labels from (C). (**E**) 3D scan of *Carcharodon carcharias* chondrocranium used to model *O. megalodon*'s head. (**F**) *C. carcharias* chondrocranium with UF 311000 dentition and IRSNB P 9893 column attached and hoops outlining the model's head. (**G**) 3D scan of the full body of the *C. carcharias* specimen used for flesh reconstruction with elliptical hooping methodology indicated for the (**H**) dorsal fin, (**I**) pectoral fins, (**J**) abdomen, (**K**) pelvic fins, and (**L**) caudal fin. (**M**) Base skeletal model with octagonal hoops that mark flesh boundaries. (**N**) Final lofted polygon mesh of *O. megalodon* used for analyses at lateral view and (**O**) dorsal view. (**P**) Visualization of open gape at 75° angle at oblique view and (**Q**) 35° gape angle at lateral view.

well as their modern relatives (see Materials and Methods; Table 2) and found that medium-size prey between 3 and 6 m (Table 2) could have been ingested in very few bites, assuming a gape angle of 75° (*7*). For example, a 5-m *P. nana*, a proposed prey of *O. megalodon* based on bite marks (*19*), could have been eaten in just three bites

according to our estimates. Larger prey of 7 to 8 m would then have had to be severed into five or more chunks. Furthermore, assuming a limit of 70% stomach fullness (*36*), we found that while complete hypothetical prey of 8 m (e.g., the size of a modern *Orcinus orca*) or less could be completely ingested, larger prey (e.g., the size of the

Table 1. Calculated properties of the completed *O. megalodon* reconstruction. COM, center of mass; DER, daily energetic requirement; TL, total length. COM axis directions are as follows: lateral (*x*); posterior (*y*); dorsal (*z*). CI = 95% confidence intervals from equations.

Property (units)	Source	Measurement	CI
TL (m)	Blender	15.9	NA
Surface area (m²)	MeshLab (*31*)	131.2	NA
Volume (m³)	MeshLab (*31*)	58.1	NA
COM *x* (m)	MeshLab (*31*)	0.2	NA
COM *y* (m)	MeshLab (*31*)	−3.3	NA
COM *z* (m)	MeshLab (*31*)	0.8	NA
Density (kg/m³)	Literature (*32*)	1,060	NA
Body mass (kg)	Eq. 1	61,560	NA
Absolute cruising speed (m/s)	Eq. 2 (*33*)	1.4	0.5–4.1
Relative cruising speed (BL/s)	Absolute speed/TL	0.09	0.03–0.26
Stomach volume (liters)	Eq. 3	9,605	8,487–10,722
Gape height 35°	Blender	1.2	NA
Gape height 75°	Blender	1.8	NA
Gape width 35°	Blender	1.7	NA
Gape width 75°	Blender	1.7	NA
DER (kcal/day)	Eq. 4 (*37*)	98,175	78,085–123,067

modern humpback whale, *M. novaeangliae*) could not. These results were also found when using the upper and lower CIs of the stomach volume estimations (Table 2); thus, subsequent interpretations were based on the mean estimate of 9605 liters.

We estimated the model's energetic demands using the previously established relationship between body mass and daily energy requirement based on 16 *C. carcharias* individuals [see Materials and Methods; (*37*)]. We found that the *O. megalodon* model required 98,175 kcal per day (95% CI = 78,085 to 123,067 kcal/day; Table 1), which is 20 times higher than that of an adult *C. carcharias* [4871 kcal for a ~900-kg individual; (*37, 38*)]. We contrasted this result against calorie-rich substances of potential prey (Table 2) to estimate the caloric contributions from prey intake while assuming 70% assimilation efficiency (*39*). Given that 30 kg of cetacean blubber contains ~200,000 kcal (*38*) based on a value of 6667 kcal/kg (*37*), a ~16-m *O. megalodon* could have met its energy demands by consuming ~21 kg of blubber per day (95% CI = 16.73 to 26.37 kg). Because 15 to 33% of a marine mammal's body is blubber (*40, 41*), approximately 81.3% of a 123-kg *X. bossi* and as little as 0.01% of a 6000-kg *O. orca* (Table 2) would have satisfied the daily calorific demands of an adult *O. megalodon*. Similarly, shark liver has been estimated to have an energy density of 8150 kcal/kg (*42*). Hence, an adult *O. megalodon* might also have met its daily energetic demands by consuming ~17.2 kg of shark liver (95% CI = 13.69 to 21.57 kg). Given that up to 28% of the body mass of *C. carcharias* is liver (*43*), an adult *O. megalodon* may have met its daily energetic demands by consuming ~1.4% of the liver of a 7-m *C. carcharias* [3271-kg body mass (*44*); 915.8-kg liver (*43*)]. Last, shark muscle has been estimated to have an energy density

of ~4400 kcal/kg in *C. carcharias* (*42*). Hence, *O. megalodon* could have met its daily energetic demands by consuming ~31.9 kg of shark muscle (95% CI = 25.35 to 39.96 kg).

We further used a random process to calculate the accumulation of net energy (*45*) to model the prey encounter rates that *O. megalodon* would have needed to sustain its population. To do so, we used (i) the 3D model's properties (Table 1), including the rate of energy expenditure; (ii) the total energy contained in the whole body of each putative prey (Table 2); and (iii) the relative abundance of such prey (table S1) (*46*). Our results indicate that if *O. megalodon* hypothetically fed exclusively on the smallest prey (e.g., 2 to 3 m; Table 2), it would have to eat, on average, once every 1.3 days to sustain its population (Fig. 3). In contrast, *O. megalodon* could have eaten only every 145 days (i.e., 5 months) if it fed exclusively on the largest prey (e.g., >12 m), while the most abundant of the putative prey (i.e., *Metaxytherium*; table S1) would have sustained *O. megalodon* for 15.5 days. Last, if it exclusively fed on the largest prey that could be completely consumed (i.e., 8 m; Table 2), the ingested energy would sustain *O. megalodon* for 63 days (2 months). This result for mean rates of prey encounter based on our probabilistic model is largely mirrored when using the ratio between energy ingested and energy expended per day.

DISCUSSION
Body size
The calculated TL (15.9 m) for the IRSNB P 9893–based 3D model is markedly longer than previously estimated for this specimen [9.2 m; (*7*)]. When scaled to real size in Blender (155 mm diameter in centrum 4; see Materials and Methods), the complete column alone was 11.1 m. Size differences likely stem from the fact that the previous estimation was based on the relationship between the largest centrum diameter and TL in *C. carcharias* and, thus, based only on centrum 4 (*7*). Nevertheless, there are some problems with the latter approach. First, it implicitly assumed that *O. megalodon* was a direct ancestor of *C. carcharias*, which is now disfavored (*30*). Second, it assumed that both species have similar vertebrae numbers and column structure (i.e., similar proportions of caudal and precaudal centra); however, the number of vertebrae varies even within members of the same family (*47*). Last, although the centrum used to estimate TL comes from an exceptionally well-preserved fossil, it is still not an entirely complete specimen (*7*); hence, it is unknown whether that was in fact the largest centrum. Larger *O. megalodon* centra have been reported elsewhere, with the largest measuring 230 mm in diameter (*16*). Our *O. megalodon* 3D reconstruction is also larger than a maximum size of 14.2 to 15.3 m previously proposed based on upper anterior teeth (*13*). The model's large size combined with the existence of known vertebral centra ~50% larger than those of IRSNB P 9893 (*16*) supports a more recent suggestion that *O. megalodon* may have reached a maximum TL of 20 m (*14*).

Our estimated body mass (61,560 kg; Table 1) was also ~23% higher than that previously inferred for a 16-m *O. megalodon* based on the relationship between TL and mass in *C. carcharias* [47,690 kg; (*7*)]. This mass difference could be due to the reliance on *C. carcharias* in previous estimates, whereas we adjusted our model to account for multiple analogs, namely, all members of the family Lamnidae (order Lamniformes; see Materials and Methods). It has been shown that incorporating multiple lamnids results in stockier *O. megalodon* body reconstructions (*15*). The use of multiple analogs to reconstruct
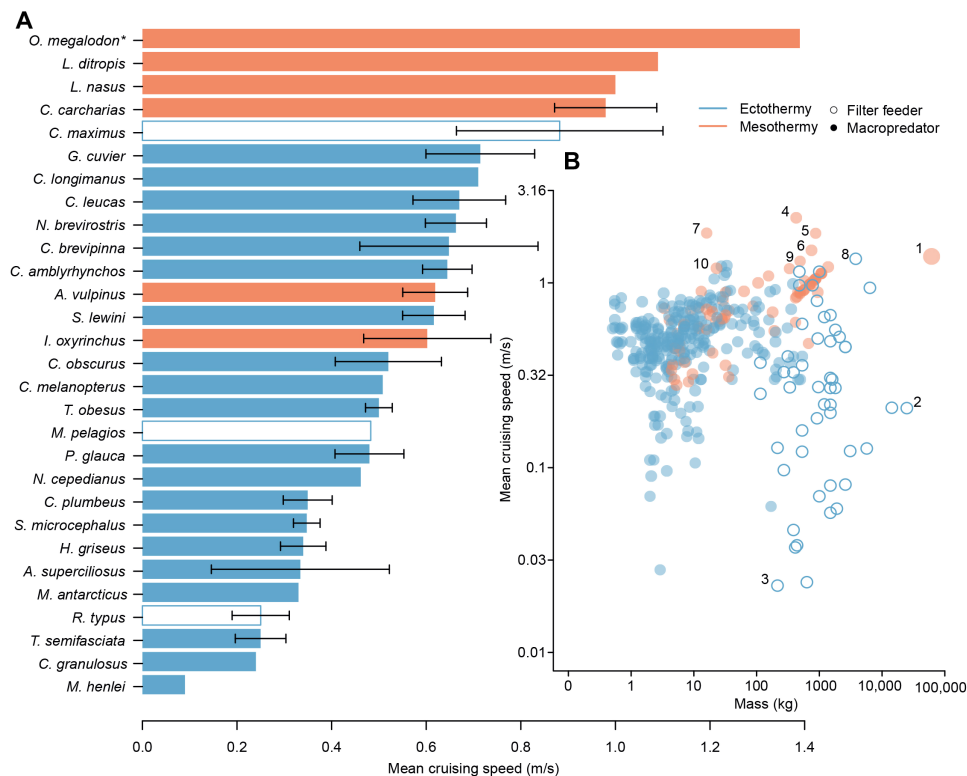
Fig. 2. Sharks' absolute cruising speeds. (**A**) Mean cruising speeds of all shark species gathered in data S1 ($n = 28$ plus the *O. megalodon* model), with error bars drawn from multiple individuals per species. An asterisk (*) indicates that *O. megalodon*'s speed estimate was made from Eq. 2 rather than from the mean of multiple speeds. Species without error bars are those from which only one individual was recorded. (**B**) Mass and mean cruising speed of all individual sharks in data S1 ($n = 392$) plotted on a log scale. Species marked are as follows: (1) *O. megalodon*, (2 and 3) the whale shark (*Rhincodon typus*), (4 to 6) the great white shark (*Carcharodon carcharias*), (7) the shortfin mako shark (*Isurus oxyrinchus*), (8) the basking shark (*Cetorhinus maximus*), (9) *C. carcharias*, and (10) *I. oxyrinchus* (see text for details of specific individuals).

the body of *O. megalodon* has recently been questioned based on a supposed lack of a relationship between body form and thermophysiology in lamniforms when analyzing drawings of all 15 extant species (*48*). Nevertheless, justification for the use of multiple analogs to reconstruct the body of *O. megalodon* is based on the combination of ecology with thermophysiology, as both ultimately determine swimming strategy and, consequently, body form in sharks (*29*, *49*). Accordingly, the analogs used to inform the reconstruction of *O. megalodon* encompass only the lamniforms that share similar diet, feeding strategy, and thermoregulatory physiologies (*15*). These include the family Lamnidae (*49–52*) but exclude ectothermic filter feeders (families Cetorhinidae and Megachasmidae) and the family Alopiidae, which includes a mesothermic species but displays anatomical adaptations (i.e., enlarged caudal fins) for a specialized hunting behavior (*53*) unlikely to be analogous to *O. megalodon* (*18–21*). Hence, the purported lack of a relationship between body form and thermophysiology in extant lamniforms based on the inclusion of species not analogous to *O. megalodon* (*48*) is not only irrelevant to the reconstruction of the extinct species as proposed in (*15*) but also at odds with previous studies demonstrating body form convergence among mesothermic taxa, including lamnid sharks, tunas (*49*, *50*), and ichthyosaurs (*54*, *55*). We therefore contend that, although *C. carcharias* is the best available ecological analog of *O. megalodon*, the use of multiple lamnids to inform our 3D reconstruction is appropriate given the uncertainties regarding the interrelationships between extinct and extant

Lamniformes (see Materials and Methods). Given that our best-case validity test suggests that our volumetric approach does not result in overestimations (see Materials and Methods), we consider a mass of 61,560 kg to be conservative to infer ecological parameters based on extant sharks. Together, our body size results suggest that the IRSNB P 9893 specimen is bigger than hitherto proposed and larger than the maximum size estimated for *O. megalodon* based on anterior teeth only (*13*). These results highlight the importance of using body parts other than anterior teeth and multiple analogs to infer the size of this extinct shark.

Movement ecology

Absolute cruising speed (m/s) estimations and species-level comparisons (Fig. 2A) suggest that the reconstructed ~16-m individual was able to cruise faster than all extant species analyzed (*33*), including its closest mesothermic, macropredatory, extant relatives. Notably, the model was also much faster than the largest extant shark species, which is the filter-feeding, ectothermic whale shark (*R. typus*; maximum size, ~18 m; Fig. 2A) (*35*). A faster cruising speed than *R. typus* was also found when considering relative speed (BL/s), a metric inversely correlated with body size (fig. S3A). It is well supported that mesothermy allows all mackerel sharks [family Lamnidae: *C. carcharias*, *Isurus* spp., and *Lamna* spp.; (*49*, *50*)] and the common thresher [*Alopias vulpinus*; (*56*)] to reach faster speeds than their ectothermic counterparts (*51*, *52*). Different lines of evidence have suggested that *O. megalodon* also had this thermoregulatory

Table 2. Body mass and volume of putative *O. megalodon* prey. Volume of each taxon is compared against the estimated stomach volume of the *O. megalodon* model (9605 liters) to determine whether it could have been completely consumed ("Complete ingestion?"). We set a limit of 70% stomach volume for full prey consumption (*36*). Energy densities for marine mammal taxa come from whole-body estimates for sirenians (1257 kcal/kg), dolphins (3052 kcal/kg), and baleen whales (7314 kcal/kg), and muscle estimates for *C. carcharias* (*42*). All literature sources for body length, body mass, and energy density can be found in table S6. Extinct taxa are denoted by daggers (†).

Taxa	Body length (m)	Body mass (kg)	Volume (liters)	Energy density (kcal/kg)	Complete ingestion?
Phocoena	2	70	71.75	3,052	Yes
†*Nanosiren*	2	150	153.75	1,257	Yes
Stenella	3	235	240.46	3,052	Yes
†*Xiphiacetus bossi*	<3.5	123	126.08	3,052	Yes
Tursiops	3.5	500	512.5	3,052	Yes
†*Orcinus* sp.	3.5	2,049	2,100.22	3,052	Yes
†*Piscobalaena nana*	<5	3,584	3,672.96	7,314	Yes
†*Carcharodon* sp.	5	1,154	1,183.02	4,400	Yes
†*Dioplotherium*	5.3	2,827	2,897.68	1,257	Yes
†*Metaxytherium*	5.7	3,492	3,579.3	1,257	Yes
Pseudorca	6	1,360	1,394	3,052	Yes
†*Balaenoptera* spp. (cortesii/bertae/davidsoni)	6	2,357	2,415.83	7,314	Yes
Globicephala	6	3,200	3,280	7,314	Yes
Delphinapterus	6	5,016	5,141.8	7,314	Yes
†*Dusisiren*	6.2	4,411	4,521.28	1,257	Yes
†*Hydrodamalis*	7	6,553	6,716.83	1,257	Yes
Carcharodon carcharias	7	3,271	3,352.54	4,400	Yes
Orcinus orca	8	6,000	6,150	3,052	Yes
Balaenoptera acutorostrata	9	8,498	8,710.51	7,314	No
Eschrichtius	>12	20,000	20,500	7,314	No
Eubalaena	>12	31,700	32,492.5	7,314	No
Balaena	>12	75,000	76,875	7,314	No
Megaptera novaeangliae	16	30,000	30,750	7,314	No

adaptation (*26*, *35*). Given that our estimated cruising speed for *O. megalodon* was based mostly on ectothermic, hence slower, species [see Materials and Methods; (*51*, *52*)], we consider it to be conservative.

The potential ability of *O. megalodon* to cruise at faster absolute speeds than other species (Fig. 2A) would enable it to move greater distances, thus increasing prey encounter rates (*51*). Fossils of marine mammals with multiple bites from the Miocene Pisco Formation of Peru have been used to hypothesize that *O. megalodon* may have exploited pinniped colonies for foraging (*19*). Hence, the ecological benefits of a faster cruising speed likely allowed *O. megalodon* to move between distant feeding sites, a predation tactic also used by *C. carcharias* to find abundant, calorie-rich prey (*57*). Overall, our species-level comparisons of absolute cruising speed suggest that *O. megalodon* was, in general, an adept swimmer capable of undertaking long migrations, perhaps even farther than extant species. In modern oceans, a *C. carcharias* swimming at a mean cruising speed of 1.3 m/s (0.1 m/s slower than *O. megalodon*) can travel as far

as 11,110 km across the entire Indian Ocean (*25*). Considering that large, highly mobile animals disproportionately drive nutrient movement between marine regions today (*58*), we propose that *O. megalodon* likely played an important ecological role transporting nutrients across oceans. Hence, the extinction of this species may have negatively affected global nutrient transfer, potentially compromising ecosystem diversity, productivity, and stability [e.g., (*58*, *59*)].

Individual-level comparisons between *O. megalodon* absolute (m/s) cruising speed with that of the 391 sharks analyzed, combined with relative cruising estimations (BL/s), provide additional clues about the biotic interactions of this extinct species. A few smaller macropredatory individuals can exceed the absolute cruising speed of a ~16-m *O. megalodon* [i.e., two adult (Fig. 2B, nos. 5 and 6) and one subadult (Fig. 2B, #4) *C. carcharias* and a juvenile *I. oxyrinchus* (Fig. 2B, no 7, and data S1)]. Similarly, the relative cruising speed (BL/s) of the *O. megalodon* model (Table 1) was found to be slower than almost all other macropredatory sharks (fig. S3). This finding is expected given the size of the model (Fig. 1) relative to extant species.
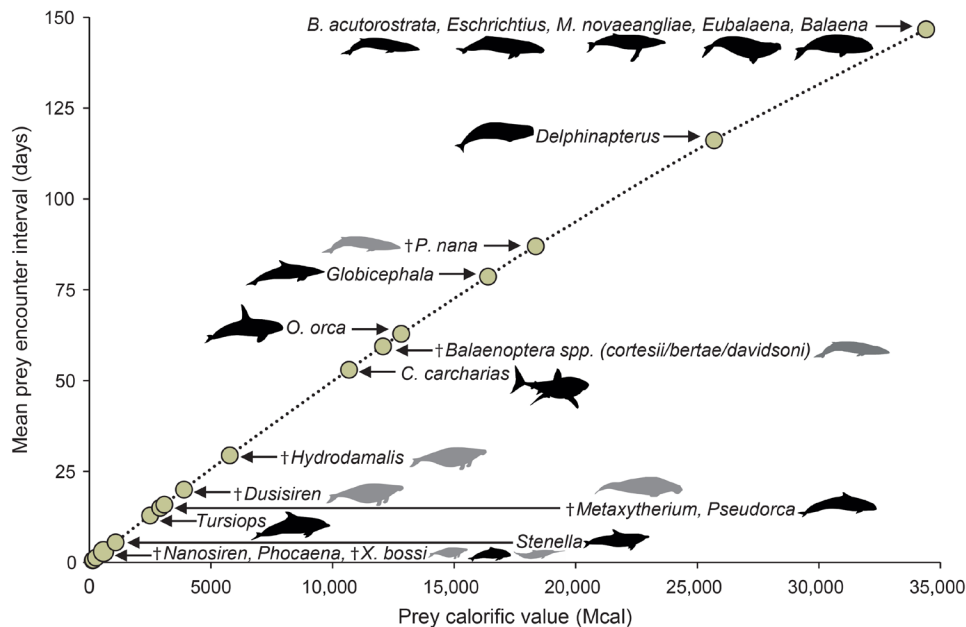
Fig. 3. Prey encounter rates. Mean required predation rate of various putative *O. megalodon* prey assuming that they are the sole food source and assuming 70% assimilation efficiency for the simulated population to be maintained (see text for details). Body mass and energy densities of all prey items are recorded in Table 2. Note that the connecting line is not linear. Dagger symbols and gray animal shapes denote extinct taxa. Black animal shapes denote extant species.

Nevertheless, when taken together, these results suggest that despite *O. megalodon*'s potential ability to move greater distances than any other species today, its gigantic size likely imposed constraints on its swimming abilities when compared to smaller macropredatory individuals. For instance, the fact that the absolute speed of a 16-m *O. megalodon* could hypothetically be exceeded by an adult *C. carcharias*, which would share a similar diet (*60*), suggests that ancient white sharks [e.g., *Carcharodon hubbelli*, a 5-m species (*14*) that overlaps with *O. megalodon* in the Pisco Formation (*30*)] could also cruise faster, potentially outcompeting it. Although this is highly speculative given that we only estimated cruising speed and not burst speed, which is directly related with prey capture (*61, 62*), it has been observed that small *C. carcharias* outcompete larger individuals using swift burst speeds when ambushing prey (*61*). Moreover, it has been previously proposed that an 18-m *O. megalodon* could reach burst speeds of 10 m/s (*26*), whereas a 3.4-m *C. carcharias* can reach at least 12 m/s (*62*). Given that body mass is curvilinearly correlated with absolute burst speed across both terrestrial and marine taxa (*34*), *O. megalodon*'s burst speed was most likely limited by the drag produced by its gigantic size (*32*). Therefore, *O. megalodon*'s maximum speed would have been attained by younger individuals, while those approaching 16 m [which is close to maximum size (*6, 14*)] would have been less agile hunters. The appearance of potential competitors in the late Miocene has already been proposed to have contributed to the extinction of *O. megalodon* in the Pliocene, in addition to habitat loss driven by sea-level oscillations and the decline of potential prey (*9–11*). Although our absolute cruising speed comparisons do not provide enough evidence to propose that ancient white sharks were able to reach faster burst speeds for swifter and more effective predatory attacks, they do imply that if *O. megalodon* faced competition, it would have been with smaller, yet adult homeothermic macropredators. Future studies considering burst speeds could

shed more light on the competitive interactions between *O. megalodon* and other sharks.

Feeding ecology

Our prey size and intake results suggest that a ~16-m *O. megalodon* could completely ingest, and in as few as five bites, prey as large as *O. orca* (i.e., 8 m), a top consumer in modern marine food webs (*63*). The macroraptorial sperm whale *Zygophyseter varolei* occupied a similar ecological niche to modern orcas in the Miocene and likely overlapped with *O. megalodon* (*64, 65*). *Z. varolei* is only known from a holotype specimen from Italy and has been estimated to reach 7 m of length (*64, 65*). Accordingly, *O. megalodon* could potentially have fully consumed this large predator. Such a predatory behavior would be similar to that of large extant predators such as *C. carcharias*, which can fully consume dolphins in two pieces (*24*). The potential ability of *O. megalodon* to fully consume large predators has two main ecological implications. First, it supports previous findings of *O. megalodon* sitting at a higher trophic level than apex predators today based on calcium isotopes (*22*), further implying an important ecological function as an apex superpredator. Second, when also considering the potential competitive interactions from our swimming speed analyses, it further suggests the possibility of a dietary preference for large prey. Although it has been previously hypothesized that *O. megalodon* preferred prey of 2 to 7 m (*19, 20*), empirical studies have shown that large sharks prey upon a broader range of sizes than their smaller counterparts (*66*). Moreover, one of the benefits of gigantism in macropredatory marine taxa is the ability to exploit less competitive niches by consuming large prey (*29, 35, 67*). For example, while toothed whales tend to feed on large patches of small prey, the largest sperm whales can acquire similar amounts of energy from eating just a few large, high-energy items (*67*). Similar energetic gains from frequent but small prey relative

to less frequent but large prey were also found in our *O. megalodon* prey encounter analysis (Fig. 3). Hence, it is possible that large *O. megalodon* individuals may have minimized competition by targeting large prey.

Our results further suggest that large prey would have provided *O. megalodon* calories well beyond its energetic demands and would have been found frequently enough to support adult populations (Fig. 3 and table S1). Although frequent predation on smaller prey such as *X. bossi* or *Metaxytherium* (Table 2) would have also sufficed *O. megalodon*'s caloric needs (Fig. 3 and table S1), it is common for large macropredatory sharks to consume far more than their required daily energy intake at a time, particularly ram-ventilating mesotherms that need to swim continuously to acquire oxygen and power metabolism (*32*, *33*, *57*). For example, adult *C. carcharias* can consume more than 30 kg of blubber from scavenging a large cetacean carcass without filling their stomachs, which is hypothesized to sustain them for up to 1.5 months, assuming continuous cruising speed (*38*). Moreover, they have been observed eating entire dolphins (*24*), which would provide up to 60 times their daily energy requirement [44 kg of blubber in a 200-kg dolphin = ~293,000 kcal (*41*)]. Prey intake beyond daily energetic demands is also common in other aquatic top predators, like polar bears (*Ursus maritimus*), which can obtain enough calories to live for up to 60 days from fully consuming an adult seal (*68*). In sharks, like *C. carcharias,* excess energy from consuming calories beyond their daily requirements is stored in liver lipids, sustaining them during prolonged migrations (*57*). This fits an established hypothesis that large mesothermic taxa have higher mass-specific metabolic limits [e.g., (*29*)], which notably lowers the cost of transport and enhances fasting capabilities (*69*). The hypothetical full consumption of a cetacean of the size of a modern *O. orca* (8 m) might have sustained a ~16-m *O. megalodon* for 63 days without jeopardizing population survival, which would have allowed it to travel over 7500 km, assuming a continuous cruising speed of 1.4 m/s. Although this suggestion is inherently inferential, it fits observations of extant species, specifically its ecological analog *C. carcharias* (*25*, *37*). Together, our results indicate that a preference for, and the full consumption of, large prey would have not only allowed *O. megalodon* to exploit less competitive niches but also potentially enabled transoceanic movements. The extinction of *O. megalodon* therefore may have released large cetaceans from a strong predatory pressure (*8*), likely affecting global trophic webs [e.g., (*59*)].

The exceptionally preserved vertebral column of the extinct giant shark *O. megalodon* from Belgium (IRSNB P 9893; Fig. 1, A and B, and fig. S1) provided a unique opportunity to reconstruct its entire body using 3D computer modeling, which in turn enabled previously unknown inferences on its movement and feeding ecology. It is important to acknowledge, however, that there are inherent uncertainties associated with any estimations of biological properties in extinct animals, which magnify when they are used as the basis for further inferences. Our conservative estimates and cautious interpretations suggest that *O. megalodon* was likely able to swim great distances and to feed on prey as large as modern apex predators, implying an ecological function as a transoceanic superpredator. A potential preference for large prey would have allowed adult individuals not only to obtain enough calories to undertake prolonged migrations, much like its modern ecological analogs (*25*, *57*), but also to exploit less competitive niches. The extinction of this purported highly migratory superpredator likely had large-scale impacts, from

releasing large cetaceans from a strong predatory pressure, thus affecting global food webs (*8*), to altering global nutrient transport, ocean productivity, and ecosystem stability (*58*).

MATERIALS AND METHODS
Fossil specimens
Vertebral column
On the basis of identical coloring and surface texture, the degree of preservation, and a gradual decrease in centrum diameter, IRSNB P 9893 is a vertebral column belonging to a single *O. megalodon* individual (*7*). This exceptional fossil specimen is stored at the Royal Belgian Institute of Natural Sciences (RBINS) in Brussels, Belgium. It was recovered from around the Antwerp basin in the 1860s (*7*); however, neither the locality nor an age has been specified beyond a Miocene range (23 to 5.3 Ma ago). The 141 centra vary in degrees of preservation from fragmentary to near complete. These centra were labeled by museum curatorial staff as "1-150" (Fig. 1A and fig. S1), although duplicated labeling or missing centra deserve consideration. Namely, there are two centra each labeled as centrum 33, 100 and 115. Moreover, centra 30, 35 to 37, 45, 105, 131, 136, 141, 146, 147, and 149 are missing from the column. These issues were accounted for during model reconstruction (see the "3D scans" section).

We measured the preserved diameter of all centra using digital calipers (data S1). As in previous studies (*7*, *17*), we observed that centrum 4 was the largest (155 mm in diameter; Fig. 1A and fig. S1) and that there is a gradual decrease in diameter toward the posterior-most section of the column, with centrum 150 being the smallest (57 mm; Fig. 1A and fig. S1). Because the largest centrum in *C. carcharias* vertebral columns is typically immediately behind the chondrocranium, Gottfried *et al.* (*7*) considered the possibility that the centra were not in the correct order. However, given the gradual decrease in centrum diameter observed in IRSNB P 9893, which has also been reported in exceptionally well-preserved columns of other extinct lamniforms (*70*), we consider it more likely that IRSNB P 9893 centra are labeled in the correct order, but the anterior-most centra are missing, an alternative also considered by Gottfried *et al.* (*7*). Despite missing anterior and caudal centra, IRSNB P 9893 is by far the most complete *O. megalodon* vertebral column known in the fossil record and serves as the basis for our 3D reconstruction.
Dentition
Teeth of *O. megalodon* are often discovered as isolated fossils. Hence, associated dentitions [i.e., where all preserved teeth belong to a single individual (*14*)] are rare. Nevertheless, there are a few such *O. megalodon* dentitions in the public record (*14*). For our reconstruction, we used a dentition (UF 311000; fig. S2) from the early Pliocene Yorktown Formation of the Lee Creek Mine in Aurora, North Carolina, United States, which is housed in the Vertebrate Paleontology Collection of the Florida Museum of Natural History (FLMNH) at the University of Florida (*14*).

3D scans
O. megalodon vertebral column
Individual centra of IRSNB P 9893 were scanned at the RBINS. Surface scans of all fossils were conducted using an HDI advanced scanner (HDI Advance R3X, LMI Technologies, Brussels, Belgium). Following scanning, the individual centrum scans were then imported into Meshmixer (http://meshmixer.com) and arranged on the basis of column position labeling. Intercentrum distances in this column

were distributed uniformly following descriptions of known shark vertebral columns in the literature [e.g., (70)]. Missing centra were accommodated by temporarily filling the space with a near-complete neighboring centrum, scaled according to its column position to ensure uniform intercentrum distances, and then removing this placeholder centrum. This was also done for fragmented centra to ensure their correct positioning. Once the column was complete, it was exported as an STL file (Fig. 1B).

O. megalodon jaws

3D scans of the UF 311000 dentition were downloaded from Morphosource (www.morphosource.org; accessed May 2015). Each tooth (Fig. 1C) was imported into Meshmixer and arranged on the basis of their known position in the jaw, as recorded by the FLMNH. Distance between teeth was inferred on the basis of known intertooth distance in jaws of *C. carcharias* (5). Given that the preservation of UF 311000 is limited almost entirely to the left side of the jaw [fig. S2; see also (14)], these teeth were mirrored around the x axis (anteroposterior) to recreate the right side of the jaw. The complete 3D dentition was exported as an STL file (Fig. 1D) and later used to reconstruct the jaw of the *O. megalodon* model.

C. carcharias specimens

We used 3D scans of two *C. carcharias* specimens to digitally reconstruct the body outline of *O. megalodon*. Although other lamnids can be considered as closely related to *O. megalodon* as *C. carcharias* (15), the latter is the largest, most well-studied species, and has the most similar dentition to *O. megalodon*. Moreover, *C. carcharias* was the one large-bodied species with an available full-body 3D scan that could be used.

The first specimen was a 3D mesh of the chondrocranium of a 2.5-m TL (240 kg) juvenile (NSWDPI-WS2006/4; Fig. 1E), which was previously modeled from computed tomography (CT) scan data to calculate the shark's bite force (71). The second was a 3D scan of the entire body of a 2.56-m TL (164 kg) juvenile female (Fig. 1F). It was retrieved by the Kwa-Zulu Natal Sharks Board (KZNSB) in November 2018 as part of its bather protection program (23). This individual was scanned on site at the KZNSB research laboratory, Umhlanga, South Africa, with a Creaform Go!Scan 3D scanner using an accuracy of 0.5 mm. Following 8 hours of digital assembly, the resulting 3D mesh was sculpted to a neutral swimming position using Rhino (www.rhino3d.com), Geomagic Design X (www.3dsystems.com/software/geomagic-design-x), and zbrush (www.Pixologic.com) software.

Model reconstruction
Skeletal model

The completed vertebral column STL file (Fig. 1B) was imported into Blender and scaled to real size based on the measured diameter of the largest centrum (centrum 4; Fig. 1A) so that the model could be recreated at the approximate size of the shark. In parallel, the scan of the *C. carcharias* chondrocranium (Fig. 1E) was imported into Meshmixer and scaled to match the size of the articulated dentition from UF 311000 (Fig. 1D). Then, the dentition was placed over the chondrocranium's teeth. The resulting mesh was exported as a single STL file and then imported into Blender, where it was scaled to fit with IRSNB P 9893 at the first vertebra. Together, the *C. carcharias* chondrocranium, UF 311000 teeth, and IRSNB P 9893 comprised the skeletal base model of the *O. megalodon* reconstruction (Fig. 1, B, D, and E).

Full-body construction

The skeletal base model was used to first recreate the head. This was done in Blender by tightly fitting octagonal hoops onto the chondrocranium and lofting them to create the final watertight mesh (Fig. 1F) using a previously established methodology (1–4). Then, the body of *C. carcharias* was used for the flesh reconstruction. To do so, we imported the full-body scan of *C. carcharias* (Fig. 1G) into Blender and scaled it so that IRSNB P 9893 ended at the base of the caudal fin. This is because the smallest centrum (#150) was proposed as being among the last of the precaudal centra (7). The octagonal hooping method used in the head was then repeated to fit tightly along the body and around each fin (Fig. 1, H to L). The skeletal base model (particularly the chondrocranium), rather than the full-body scan of the *C. carcharias*, was used to reconstruct the *O. megalodon*'s head because a watertight mesh requires symmetry for more accurate mass estimates (2), which the full-body *C. carcharias* head did not have. Consequently, our reconstruction of the head is slightly undersized. The resulting hoops around the chondrocranium, vertebral column, and full-body *C. carcharias* produced the outline of our *O. megalodon* model, and all were lofted together to form the shark's flesh (Fig. 1M).

Model adjustment

We adjusted the dimensions of the initial *O. megalodon* model based on a previous 2D reconstruction that was built using all lamnid species as analogs (15). The selection of analogs was based on both ecological and thermophysiological similarities among extant relatives (15). The use of these analogs was further justified on the basis of quantitative evidence for isometry between body parts ($n = 24$) with respect to TL within and among laminds using photographic data from 41 individuals at different life stages (15). This was done for three reasons: (i) Despite *C. carcharias* being considered the best modern analog of *O. megalodon* (7, 13), there are uncertainties regarding the interrelationships between extinct and extant Lamniformes, and therefore, *O. megalodon* could be as closely related to *C. carcharias* as to any other lamniform (35); (ii) the previous 2D reconstruction of *O. megalodon* showed that relying solely on *C. carcharias* results in a more slender body (i.e., narrower vertical dimensions) than when also using similarly related lamniform analogs (15); and (iii) the *C. carcharias* scans used to complete the model were juveniles, and our skeletal model based on IRSNB P 9893 was an adult. Only two vertical dimensions (dorsal tip to abdomen and dorsal posterior to abdomen; table S2) required adjusting, as they were initially close to the minimum estimated values. Last, we used this 2D model (15) to aid the reconstruction of the anal fin, which was the only fin not captured in the scan of *C. carcharias*, likely due to how the shark was positioned during scanning. To recreate this fin, we duplicated the *O. megalodon* model's dorsal fin, mirrored it around the z axis (mediolateral), and scaled it down to match the size, shape, and positioning of this fin in the 2D reconstruction (15). These steps concluded the reconstruction of the model, which once completed was used for all subsequent analyses (Fig. 1, N to Q). A detailed guide of the model reconstruction procedure can be found in the Dryad Data Repository.

Model measurements

The TL of the completed model was measured in Blender (Table 1). Then, the model mesh (Fig. 1, N and O, and data S2) was exported as an STL file and imported into MeshLab (31), where it was cleaned and simplified. Then, the "Compute Geometrics Measures" filter

was applied, which produced mesh surface area, volume (*V*), and center of mass (COM). To calculate the model polygonal mesh's body mass (*M*), we combined *V* with density (*D*), as performed in previous studies (*1*, *3*, *4*). The density of sharks is widely accepted as being only slightly higher than that of seawater (*43*, *72*). In pelagic sharks, this has been found to be an average of around 1060 kg/m³ (*32*). We therefore applied this same density value to the *O. megalodon* model. The resulting equation used to calculate mass is as follows

$$M \,(\text{kg}) = V \,(\text{m}^3) * D \left(\frac{\text{kg}}{\text{m}^3} \right) \tag{1}$$

We measured the gape height (maximum distance between upper and lower jaws) and width (distance between left and right edges of the mouth) of the model in Blender at 35° and 75° angles (fig. S4). The 35° gape angle was assumed because it has been previously used to calculate bite force in *C. carcharias* and, subsequently, *O. megalodon* (*71*). Similarly, the 75° gape angle was used because it is among the largest gape sizes observed in *C. carcharias* and was used in a previous reconstruction of *O. megalodon* based on IRSNB P 9893 (*7*). We therefore consider 75° to be a conservative gape angle because large sharks typically exhibit wider gapes than small sharks as they consume larger prey (*73*). Nevertheless, we do not propose 75° as a maximum gape angle considering that estimating maximum gape size or precise kinematics (*74*) without a preserved chondrocranium would be highly speculative. We recreated the model *O. megalodon* exhibiting these open gapes (Fig. 1, P and Q) by using the same hoop-based methodology (*1*–*4*) as in the original model (Fig. 1, F to M, and movie S1).

Best-case validity test
To test the validity of the method used to calculate the model's body mass, we imported the full-body *C. carcharias* 3D scan (Fig. 1G) into MeshLab (*31*) and calculated its volume (0.13 m³), surface area (2.5 m²), and COM (*x* = 0.59; *y* = 0.03; *z* = 0.57). We then applied Eq. 1 and compared this result against the mass measured empirically of this individual (=164 kg). We found that the mass resulting from the 3D scan was 135.4 kg, which is ~18% lower than the individual's empirically calculated mass. This underestimation might be due to the fact that the anal fin was not captured by the scan and/or by postmortem processes taking place between capture and measurements in the laboratory.

Ecological estimations
Cruising speed
We used the calculated *M* to estimate the model's mean cruising speed (*S*). We did so by using the equation proposed in (*33*)

$$S \,(\text{m/s}) = 0.266 \, M \,(\text{kg})^{0.15} \tag{2}$$

Equation 2 was based on empirical data from 26 mesothermic, but mostly ectothermic, extant shark species from 64 studies (*33*). The exponent of 0.15 is derived from a theoretical model that incorporates metabolism into the scaling relationship while correcting for phylogeny (at the order level). The 0.266 constant comes from fitting the power equation to the untransformed data from the 26 species while accounting for trophic level, habitat type, and temperature [table S3 and data S1; (*33*)]. To estimate a possible range of cruising speeds for *O. megalodon*, we applied Eq. 2 using the lower and upper limit of the 95% CIs of the 0.15 exponent [95% CI = 0.053

to 0.249; (*33*)]. To calculate the model's relative cruising speed, we divided its absolute cruising speed by its TL (recorded in meters; note that TL is used here as BL). Once the cruising speed of *O. megalodon* was estimated, we included it in the dataset from (*33*) to compare it with other shark species. We did so by searching the 64 studies comprising this dataset to gather the TL, body mass, and mean cruising speed (both absolute and relative) of each individual recorded. For studies where only body length measurements were reported, we determined body mass using length-weight power equations from FishBase (*75*). We added two additional extant species to the species dataset: the Greenland shark (*Somniosus microcephalus*), due to its large size, and the spinner shark (*Carcharhinus brevipinna*), as it is larger than many of its relatives included in the dataset (*53*). In total, we collated the mean cruising speeds of 391 individuals representing 28 extant shark species.

Stomach volume
Twelve *C. carcharias* individuals from the KZNSB bather protection program (*23*) were weighed and then dissected, and their stomachs were removed with the duodenum and esophagus attached. Stomach contents were removed, and cable ties were used to close the pyloric sphincter. Each stomach was suspended by the esophagus and filled with water up to the cardia, with the resulting volume being measured to the nearest centiliter (table S4). The linear relationship between *M* and *SV* (stomach volume) ($R^2 = 0.974$) was recorded as follows

$$SV \,(\text{L}) = 0.15613 \, M \,(\text{kg}) - 6.54137 \tag{3}$$

Of the 12 *C. carcharias* individuals examined, 11 were juveniles and the other was a subadult. However, the relationship between *SV* and *M* in this species has been found to be isometric (*37*), indicating that they grow at similar rates throughout ontogeny. The presence of entire prey items, not necessarily fully intact, such as small sharks or dolphins, within *C. carcharias* stomachs (*23*, *24*) has been previously used to justify the accuracy of this relationship (*37*). Given that isometric scaling relationships between body parts have been found in different lamnid species and used to infer the dimensions of *O. megalodon* (*15*), we used Eq. 3 to estimate the mesh model's *SV*. To account for the uncertainties that arise from estimating properties of an extinct species, 95% CIs were calculated for each of Eq. 3's components (table S5) to obtain a lower and upper limit of *SV*.

Prey size
To further infer the size of prey items that *O. megalodon* could consume, we collected from the literature the body length and mass of various potential and hypothetical prey, encompassing a wide range of body sizes. These included (i) extinct taxa that have likely been preyed on by *O. megalodon* based on fossil evidence [e.g., *X. bossi* and *P. nana*; (*19*, *20*)], (ii) taxa that could have overlapped in time (Miocene and/or Pliocene epochs) with *O. megalodon* at genus level [e.g., *Carcharodon*, *Orcinus*, and *Megaptera*; (*11*)], and (iii) extant species belonging to these genera (Table 2). We compared the length of each putative prey against the calculated gape width. We also calculated the volume of each prey by dividing its body mass (kilograms) by the approximate density of water (1000 kg/m³) and converting from cubic meters to liters. This volume was then multiplied by 1.025 to account for the specific gravity of sea water (*72*). The results were compared against the stomach volume calculated for the *O. megalodon* model to determine whether this shark could have entirely consumed each taxon. Given that *O. megalodon* stomach

is unlikely to have ever been completely full because stomach acids, digestive enzymes, and accidently ingested seawater occupy stomach space (76), we limited the maximum mass/volume of prey to 70% of *O. megalodon* stomach volume based on data from extant sharks (36).

Daily energy requirement

Body mass, thermoregulation, and energetic requirements are closely associated with metabolism (49). Notably, it has been proposed that *C. carcharias* has a similar metabolic rate to endothermic mammals and birds (37). This is a result of its mesothermy (49), an ability assumed to have also evolved in *O. megalodon* (26, 29, 35). One of the proposed advantages of this physiological adaptation, in addition to elevated cruising speeds, is niche expansion, as it allows sharks to tolerate a greater range of temperatures [(51); but see (52)]. This is apparent in *C. carcharias*, which has a worldwide distribution across both temperate and tropical waters (53), and has been recorded migrating across entire oceans (25). Biogeographic analyses of fossil occurrences have suggested that *O. megalodon* also occupied a worldwide geographical range, supporting similar metabolic demands and thermoregulation (9).

Our calculation of the model's daily energetic requirement (*DER*) was based on a previous work that used the body mass and cruising speeds of 16 *C. carcharias* individuals of different sizes to estimate their daily red muscle heat production (37). As ram ventilators must continuously swim, it is generally assumed that the heat produced from a day's average cruising speed matches resting metabolic rate (37, 38, 77). Heat production is then transformed into energy production (in kilocalories), with the energy produced in a day assumed to be the minimum requirement (37). Heat production estimates from this study (37) coincide closely with the temperature of the tissue adjacent to red muscles of adult *C. carcharias* observed in the field (38, 78), as well as metabolic rates calculated from oxygen consumption in both captive neonates (77) and a field-observed adult individual (38). Given that *O. megalodon* was likely mesothermic (26, 35), it would have had a metabolic rate comparable with that of other mesothermic sharks such as *C. carcharias* (38, 77). Hence, to calculate *O. megalodon*'s *DER*, we applied the following equation based on the *C. carcharias* heat production model as proposed in (37)

$$DER \left(\frac{\text{kcal}}{\text{day}}\right) = 37.405 \, M \, (\text{kg})^{0.7139} \tag{4}$$

As in both *S* and *SV*, we used 95% CIs to account for uncertainties. Previous work on *C. carcharias* provided standard errors (SEs) for Eq. 4's constant and exponent (±1.04 and ±0.008, respectively) (37). We thus calculated CIs from those SEs (1.96*SE; CI = ±2.0384 and ±0.01568, respectively) and applied them to Eq. 4 to provide lower and upper limits of *O. megalodon* daily energy requirement.

Prey encounter rate

The ability of *O. megalodon* to meet its *DER* likely depended not only on prey size and energy content but also on how frequently it encountered such prey. We modeled *O. megalodon* food encounter rates for a hypothetical population, which followed each individual over an extended time period. Our model used a constant probability that animals would find food for any time spent foraging but incorporated a rate of decline of energy reserves for both foraging and nonforaging periods. Thus, our model, which was based on a random process to calculate the net energy accumulated (45), estimated the mean encounter rates necessary for a population to survive while accounting for the variability that scarce food sources engender in

feeding frequency across populations and, therefore, the nutritional state of all individuals within that population (79). To populate this model, we used energy densities and mean mass of putative prey from literature (Table 2) to calculate the total energy available from each prey. We then subjected total energy figures to an assimilation efficiency of 70% (39) to derive a final value for available energy per prey item. We also assumed that the shark foraged for 50% of the time, spending its calculated daily energy requirement (Eq. 4). To access the necessary mean encounter rate, for any given prey, we iteratively changed the probability of prey encounter per hour spent foraging until a population of 10,000 *O. megalodon* sharks: (i) maintained their average body mass over a complete year [see (46) for an extended time-based analysis of the consequences of probabilistic prey encounter], while (ii) no more than 5% of the population lost more than 30% of their body mass [because maximum body mass loss in sharks before death is ca. 35% (80)]. We also determined which putative prey would have been most abundant based on fossil occurrence data gathered from the Palaeobiology Database (http://paleodb.org, accessed April 2021; table S1) to assess the probabilities of encountering such prey. Probabilities, normally defined as a number between 0 and 1 per unit time (79), were, for convenience, expressed as the mean number of days over which all sharks had to forage for the survival criteria listed above to be fulfilled.

SUPPLEMENTARY MATERIALS

Supplementary material for this article is available at https://science.org/doi/10.1126/sciadv.abm9424

REFERENCES AND NOTES

1. J. R. Hutchinson, V. Ng-Thow-Hing, F. C. Anderson, A 3D interactive method for estimating body segmental parameters in animals: Application to the turning and running performance of *Tyrannosaurus rex*. *J. Theor. Biol.* **246**, 660–680 (2007).
2. V. Allen, H. Paxton, J. R. Hutchinson, Variation in center of mass estimates for extant sauropsids and its importance for reconstructing inertial properties of extinct archosaurs. *Anat. Rec.* **292**, 1442–1461 (2009).
3. K. T. Bates, P. L. Manning, D. Hodgetts, W. I. Sellers, Estimating mass properties of dinosaurs using laser imaging and 3D computer modelling. *PLOS ONE* **4**, e4532 (2009).
4. J. R. Hutchinson, K. T. Bates, J. Molnar, V. Allen, P. J. Makovicky, A computational analysis of limb and body dimensions in *Tyrannosaurus rex* with implications for locomotion, ontogeny, and growth. *PLOS ONE* **6**, e26037 (2011).
5. G. Hubbell, Using tooth structure to determine the evolutionary history of the white shark, in *Great White Sharks: The Biology of* Carcharodon carcharias, A. P. Klimley, D. G. Ainley, Eds. (Academic Press, 1996), pp. 9–18.
6. C. Pimiento, M. A. Balk, Body-size trends of the extinct giant shark *Carcharocles megalodon*: A deep-time perspective on marine apex predators. *Paleobiology* **41**, 479–490 (2015).
7. M. D. Gottfried, L. J. V. Compagno, S. C. Bowman, Size and skeletal anatomy of the giant "megatooth" shark *Carcharodon megalodon*, in *Great White Sharks: The Biology of* Carcharodon carcharias, A. P. Klimley, D. G. Ainley, Eds. (Academic Press, 1996), pp. 55–66.
8. C. Pimiento, C. F. Clements, When did *Carcharocles megalodon* become extinct? A new analysis of the fossil record. *PLOS ONE* **9**, e111086 (2014).
9. C. Pimiento, B. J. MacFadden, C. F. Clements, S. Varela, C. Jaramillo, J. Velez-Juarbe, B. R. Silliman, Geographical distribution patterns of *Carcharocles megalodon* over time reveal clues about extinction mechanisms. *J. Biogeogr.* **43**, 1645–1655 (2016).
10. R. W. Boessenecker, D. J. Ehret, D. J. Long, M. Churchill, E. Martin, S. J. Boessenecker, The early Pliocene extinction of the mega-toothed shark *Otodus megalodon*: A view from the eastern North Pacific. *PeerJ* **7**, e6088 (2019).
11. C. Pimiento, J. N. Griffin, C. F. Clements, D. Silvestro, S. Varela, M. D. Uhen, C. Jaramillo, The Pliocene marine megafauna extinction and its impact on functional diversity. *Nat. Ecol. Evol.* **1**, 1100–1106 (2017).
12. K. Shimada, The relationship between the tooth size and total body length in the white shark. *J. Fossil Res.* **35**, 28–33 (2003).
13. K. Shimada, The size of the megatooth shark, *Otodus megalodon* (Lamniformes: Otodontidae), revisited. *Hist. Biol.* **33**, 904–911 (2019).

14. V. J. Perez, R. M. Leder, T. Badaut, Body length estimation of Neogene lamniform sharks (*Carcharodon* and *Otodus*) derived from associated dentitions. *Palaeontol. Electron.* **24**, a09 (2021).

15. J. A. Cooper, C. Pimiento, H. G. Ferrón, M. J. Benton, Body dimensions of the extinct giant shark *Otodus megalodon*: A 2D reconstruction. *Sci. Rep.* **10**, 14596 (2020).

16. S. E. Bendix-Almgreen, *Carcharodon megalodon* from the Upper Miocene of Denmark, with comments on elasmobranch tooth enameloid: Coronoïn. *Bull. Geol. Soc. Denmark* **32**, 1–32 (1983).

17. K. Shimada, M. F. Bonnan, M. A. Becker, M. L. Griffiths, Ontogenetic growth pattern of the extinct megatooth shark *Otodus megalodon*—Implications for its reproductive biology, development, and life expectancy. *Hist. Biol.* **33**, 3254–3259 (2021).

18. R. J. Kallal, S. J. Godfrey, D. J. Ortner, Bone reactions on a Pliocene cetacean rib indicate short-term survival of predation event. *Int. J. Osteoarchaeol.* **22**, 253–260 (2010).

19. A. Collareta, O. Lambert, W. Landini, C. Di Celma, E. Malinverno, R. Varas-Malca, M. Urbina, G. Bianucci, Did the giant extinct shark *Carcharocles megalodon* target small prey? Bite marks on marine mammal remains from the late Miocene of Peru. *Palaeogeogr. Palaeoclimatol. Palaeoecol.* **469**, 84–91 (2017).

20. S. J. Godfrey, M. Ellwood, S. Groff, M. S. Verdin, *Carcharocles*-bitten Odontocete caudal vertebrae from the Coastal Eastern United States. *Acta Palaeontol. Pol.* **63**, 463–468 (2018).

21. S. J. Godfrey, J. R. Nance, N. L. Riker, *Otodus*-bitten sperm whale tooth from the Neogene of the Coastal Eastern United States. *Acta Palaeontol. Pol.* **66**, 599–603 (2021).

22. J. E. Martin, T. Tacail, S. Adnet, C. Girard, V. Balter, Calcium isotopes reveal the trophic position of extant and fossil elasmobranchs. *Chem. Geol.* **415**, 118–125 (2015).

23. G. Cliff, S. F. J. Dudley, B. Davis, Sharks caught in the protective gill nets off Natal, South Africa. 2. The great white shark *Carcharodon carcharias* (Linnaeus). *S. Afr. J. Mar. Sci.* **8**, 131–144 (1989).

24. I. K. Fergusson, Distribution and autoecology of the white shark in the Eastern North Atlantic and the Mediterranean Sea, in *Great White Sharks: The Biology of* Carcharodon carcharias, A. P. Klimley, D. G. Ainley, Eds. (Academic Press, 1996), pp. 321–345.

25. R. Bonfil, M. Meÿer, M. C. Scholl, R. Johnson, S. O'Brien, H. Oosthuizen, S. Swanson, D. Kotze, M. Paterson, Transoceanic migration, spatial dynamics, and population linkages of white sharks. *Science* **310**, 100–103 (2005).

26. H. G. Ferrón, Regional endothermy as a trigger for gigantism in some extinct macropredatory sharks. *PLOS ONE* **12**, e0185185 (2017).

27. D. M. P. Jacoby, P. Siriwat, R. Freeman, C. Carbone, Correction to 'Is the scaling of swim speed in sharks driven by metabolism?'. *Biol. Lett.* **12**, 20160775 (2016).

28. K. A. Dickson, J. B. Graham, Evolution and consequences of endothermy in fishes. *Physiol. Biochem. Zool.* **77**, 998–1018 (2004).

29. H. G. Ferrón, C. Martínez-Pérez, H. Botella, The evolution of gigantism in active marine predators. *Hist. Biol.* **30**, 712–716 (2017).

30. D. J. Ehret, B. J. MacFadden, D. S. Jones, T. J. Devries, D. A. Foster, R. Salas-Gismondi, Origin of the white shark *Carcharodon* (Lamniformes: Lamnidae) based on recalibration of the Upper Neogene Pisco Formation of Peru. *Palaeontology* **55**, 1139–1153 (2012).

31. P. Cignoni, M. Callieri, M. Corsini, M. Dellepiane, F. Ganovelli, G. Ranzuglia, Meshlab: An open-source mesh processing tool, in *Eurographics Italian Chapter Conference* (The Eurographics Association, 2008), pp. 129–136.

32. A. C. Gleiss, J. Potvin, J. A. Goldbogen, Physical trade-offs shape the evolution of buoyancy control in sharks. *Proc. R. Soc. B* **284**, 20171345 (2017).

33. D. M. P. Jacoby, P. Siriwat, R. Freeman, C. Carbone, Is the scaling of swim speed in sharks driven by metabolism? *Biol. Lett.* **11**, 20150781 (2015).

34. M. R. Hirt, W. Jetz, B. C. Rall, U. Brose, A general scaling law reveals why the largest animals are not the fastest. *Nat. Ecol. Evol.* **1**, 1116–1122 (2017).

35. C. Pimiento, J. L. Cantalapiedra, K. Shimada, D. J. Field, J. B. Smaers, Evolutionary pathways toward gigantism in sharks and rays. *Evolution* **73**, 588–599 (2019).

36. W. N. Joyce, S. E. Campana, L. J. Natanson, N. E. Kohler, H. L. Pratt Jr., C. F. Jensen, Analysis of stomach contents of the porbeagle shark (*Lamna nasus* Bonnaterre) in the northwest Atlantic. *ICES J. Mar. Sci.* **59**, 1263–1269 (2002).

37. D. C. Bernvi, "Ontogenetic influences on endothermy in the great white shark (*Carcharodon carcharias*)," thesis, Stockholm University (2016).

38. F. G. Carey, J. W. Kanwisher, O. Brazier, G. Gabrielson, J. G. Casey, H. L. Pratt Jr., Temperature and activities of a white Shark, Carcharodon carcharias. *Copeia* **1982**, 254–260 (1982).

39. S. C. Leigh, Y. Papastamatiou, D. P. German, The nutritional physiology of sharks. *Rev. Fish Biol. Fish.* **27**, 561–585 (2017).

40. C. Lockyer, Body weights of some species of large whales. *ICES J. Mar. Sci.* **36**, 259–273 (1976).

41. D. J. Struntz, W. A. McLellan, R. M. Dillaman, J. E. Blum, J. R. Kucklick, D. A. Pabst, Blubber development in bottlenose dolphins (*Tursiops truncatus*). *J. Morphol.* **259**, 7–20 (2004).

42. H. R. Pethybridge, C. C. Parrish, B. D. Bruce, J. W. Young, P. D. Nichols, Lipid, fatty acid and energy density profiles of white sharks: Insights into the feeding ecology and ecophysiology of a complex top predator. *PLOS ONE* **9**, e97877 (2014).

43. T. Lingham-Soliar, Caudal fin allometry in the white shark *Carcharodon carcharias*: Implications for locomotory performance and ecology. *Naturwissenschaften* **92**, 231–236 (2005).

44. H. F. Mollet, G. M. Cailliet, Using allometry to predict body mass from linear measurements of the white shark, in *Great White Sharks: The Biology of* Carcharodon carcharias, A. P. Klimley, D. G. Ainley, Eds. (Academic Press, 1996), pp. 81–89.

45. D. W. Stephens, E. L. Charnov, Optimal foraging: Some simple stochastic models. *Behav. Ecol. Sociobiol.* **10**, 251–263 (1982).

46. R. P. Wilson, M. D. Holton, A. Neate, M. Del'Caño, F. Quintana, K. Yoda, A. Gómez-Laich, Luck and tactics in foraging success: The case of the imperial shag. *Mar. Ecol. Prog. Ser.* **682**, 1–12 (2022).

47. B. W. Kent, The cartilaginous fishes (chimaeras, sharks and rays) of Calvert Cliffs, Maryland, USA, in *The Geology and Vertebrate Paleontology of Calvert Cliffs, Maryland, USA*, S. J. Godfrey, Ed. (Smithsonian Institution Scholarly Press, 2018), pp. 45–157.

48. P. C. Sternes, J. J. Wood, K. Shimada, Body forms of extant lamniform sharks (Elasmobranchii: Lamniformes), and comments on the morphology of the extinct megatooth shark, *Otodus megalodon*, and the evolution of lamniform thermophysiology. *Hist. Biol.* 1–13 (2022).

49. D. Bernal, K. A. Dickson, R. E. Shadwick, J. B. Graham, Review: Analysis of the evolutionary convergence for high performance swimming in lamnid sharks and tunas. *Comp. Biochem. Physiol. A Mol. Integr. Physiol.* **129**, 695–726 (2001).

50. J. M. Donley, C. A. Sepulveda, P. Konstantinidis, S. Gemballa, R. E. Shadwick, Convergent evolution in mechanical design of lamnid sharks and tunas. *Nature* **429**, 61–65 (2004).

51. Y. Y. Watanabe, K. J. Goldman, J. E. Caselle, D. D. Chapman, Y. P. Papastamatiou, Comparative analyses of animal-tracking data reveal ecological significance of endothermy in fishes. *Proc. Natl. Acad. Sci. U.S.A.* **112**, 6104–6109 (2015).

52. L. Harding, A. Jackson, A. Barnett, I. Donohue, L. Halsey, C. Huveneers, C. Meyer, Y. Papastamatiou, J. M. Semmens, E. Spencer, Y. Watanabe, N. Payne, Endothermy makes fishes faster but does not expand their thermal niche. *Funct. Ecol.* **35**, 1951–1959 (2021).

53. D. A. Ebert, S. L. Fowler, L. J. V. Compagno, *Sharks of the World: A Fully Illustrated Guide* (Wild Nature Press, 2013).

54. T. Lingham-Soliar, Convergence in thunniform anatomy in lamnid sharks and Jurassic ichthyosaurs. *Integr. Comp. Biol.* **56**, 1323–1336 (2016).

55. A. Bernard, C. Lécuyer, P. Vincent, R. Amiot, N. Bardet, E. Buffetaut, G. Cuny, F. Fourel, F. Martineau, J. Mazin, A. Prieur, Regulation of body temperature by some Mesozoic marine reptiles. *Science* **328**, 1379–1382 (2010).

56. D. Bernal, C. A. Sepulveda, Evidence for temperature elevation in the aerobic swimming musculature of the common thresher shark, *Alopias vulpinus*. *Copeia* **2005**, 146–151 (2005).

57. G. Del Raye, S. J. Jorgensen, K. Krumhansl, J. M. Ezcurra, B. A. Block, Travelling light: White sharks (*Carcharodon carcharias*) rely on body lipid stores to power ocean-basin scale migration. *Proc. R. Soc. B* **280**, 20130836 (2013).

58. C. E. Doughty, J. Roman, S. Faurby, A. Wolf, A. Haque, E. S. Bakker, Y. Malhi, J. B. Dunning Jr., J. -C. Svenning, Global nutrient transport in a world of giants. *Proc. Natl. Acad. Sci. U.S.A.* **113**, 868–873 (2016).

59. R. A. Myers, J. K. Baum, T. D. Shepherd, S. P. Powers, C. H. Peterson, Cascading effects of the loss of apex predatory sharks from a coastal ocean. *Science* **315**, 1846–1850 (2007).

60. C. G. Diedrich, Evolution of white and megatooth sharks, and evidence for early predation on seals, sirenians, and whales. *Nat. Sci.* **5**, 1203–1218 (2013).

61. R. A. Martin, N. Hammerschlag, R. S. Collier, C. Fallows, Predatory behaviour of white sharks (*Carcharodon carcharias*) at Seal Island, South Africa. *J. Mar. Biol. Assoc. U.K.* **85**, 1121–1135 (2005).

62. R. A. Martin, N. Hammerschlag, Marine predator–prey contests: Ambush and speed versus vigilance and agility. *Mar. Biol. Res.* **8**, 90–94 (2012).

63. S. J. Jorgensen, S. Anderson, F. Ferretti, J. R. Tietz, T. Chapple, P. Kanive, R. W. Bradley, J. H. Moxley, B. A. Block, Killer whales redistribute white shark foraging pressure on seals. *Sci. Rep.* **9**, 6153 (2019).

64. G. Bianucci, W. Landini, Killer sperm whale: A new basal physeteroid (Mammalia, Cetacea) from the Late Miocene of Italy. *Zool. J. Linn. Soc.* **148**, 103–131 (2006).

65. E. Peri, P. L. Falkingham, A. Collareta, G. Bianucci, Biting in the Miocene seas: Estimation of the bite force of the macroraptorial sperm whale *Zygophyseter varolai* using finite element analysis. *Hist. Biol.* 1–12 (2021).

66. L. O. Lucifora, V. B. García, R. C. Menni, A. H. Escalante, N. M. Hozbor, Effects of body size, age and maturity stage on diet in a large shark: Ecological and applied implications. *Ecol. Res.* **24**, 109–118 (2009).

67. J. A. Goldbogen, D. E. Cade, D. M. Wisniewska, J. Potvin, P. S. Segre, M. S. Savoca, E. L. Hazen, M. F. Czapanskiy, S. R. Kahane-Rapport, S. L. DeRuiter, S. Gero, P. Tønnesen, W. T. Gough, M. B. Hanson, M. M. Holt, F. H. Jensen, M. Simon, A. K. Stimpert, P. Arranz, D. W. Johnston, D. P. Nowacek, S. E. Parks, F. Visser, A. S. Friedlaender, P. L. Tyack, P. T. Madsen, N. D. Pyenson, Why whales are big but not bigger: Physiological drivers and ecological limits in the age of ocean giants. *Science* **366**, 1367–1372 (2019).

68. A. M. Pagano, T. M. Williams, Physiological consequences of Arctic sea ice loss on large marine carnivores: Unique responses by polar bears and narwhals. *J. Exp. Biol.* **224**, jeb228049 (2021).

69. J. A. Goldbogen, Physiological constraints on marine mammal body size. *Proc. Natl. Acad. Sci. U.S.A.* **115**, 3995–3997 (2018).

70. J. Kriwet, H. Mewis, O. Hampe, A partial skeleton of a new lamniform mackerel shark from the Miocene of Europe. *Acta Palaeontol. Pol.* **60**, 857–875 (2014).

71. S. Wroe, D. R. Huber, M. Lowry, C. McHenry, K. Moreno, P. Clausen, T. L. Ferrara, E. Cunningham, M. N. Dean, A. P. Summers, Three-dimensional computer analysis of white shark jaw mechanics: How hard can a great white bite? *J. Zool.* **276**, 336–342 (2008).

72. A. Larramendi, G. S. Paul, S.-Y. Hsu, A review and reappraisal of the specific gravities of present and past multicellular organisms, with an emphasis on tetrapods. *Anat. Rec.* **304**, 1833–1888 (2020).

73. T. L. Ferrara, P. Clausen, D. R. Huber, C. R. McHenry, V. Peddemors, S. Wroe, Mechanics of biting in great white and sandtiger sharks. *J. Biomech.* **44**, 430–435 (2011).

74. C. D. Wilga, P. J. Motta, C. P. Sanford, Evolution and ecology of feeding in elasmobranchs. *Integr. Comp. Biol.* **47**, 55–69 (2007).

75. R. Froese, D. Pauly, FishBase World wide web electronic publication, version (01/2017); www.fishbase.org [accessed June 2020].

76. T. Kubodera, H. Watanabe, T. Ichii, Feeding habits of the blue shark, *Prionace glauca*, and salmon shark, *Lamna ditropis*, in the transition region of the Western North Pacific. *Rev. Fish Biol. Fish.* **17**, 111–124 (2006).

77. J. M. Ezcurra, C. G. Lowe, H. F. Mollet, L. A. Ferry, J. B. O'Sullivan, Oxygen consumption rate of young-of-the-year white sharks, *Carcharodon carcharias*, during transport to the Monterey Bay aquarium, in *Global Perspectives on the Biology and Life History of the Great White Shark*, M. L. Domeier, Ed. (CRC Press, 2012), pp. 17–25.

78. T. C. Tricas, J. E. McCosker, Predatory behavior of the white shark (*Carcharodon carcharias*), with notes on its biology. *Proc. Calif. Acad. Sci.* **43**, 221–238 (1984).

79. R. P. Wilson, A. Neate, M. D. Holton, E. L. C. Shepard, D. M. Scantlebury, S. A. Lambertucci, A. di Virgilio, E. Crooks, C. Mulvenna, N. Marks, Luck in food finding affects individual performance and population trajectories. *Curr. Biol.* **28**, 3871–3877.e5 (2018).

80. K. O. Lear, D. L. Morgan, J. M. Whitty, N. M. Whitney, E. E. Byrnes, S. J. Beatty, A. C. Gleiss, Divergent field metabolic rates highlight the challenges of increasing temperatures and energy limitation in aquatic ectotherms. *Oecologia* **193**, 311–323 (2020).

81. E. Nordøy, L. Folkow, P.-E. Mtensson, A. Blix, Food requirements of Northeast Atlantic minke whales, in *Developments in Marine Biology* (Elsevier, 1995), pp. 307–317.

82. P. C. Valery, T. Ibiebele, M. Harris, A. C. Green, A. Cotterill, A. Moloney, A. K. Sinha, G. Garvey, Diet, physical activity, and obesity in school-aged indigenous youths in northern Australia. *J. Obes.* **2012**, 1–12 (2012).

83. B. Davidson, G. Cliff, Comparison of pinniped and cetacean prey tissue lipids with lipids of their elasmobranch predator. *In Vivo* **28**, 223–228 (2014).

84. W. A. McLellan, H. N. Koopman, S. A. Rommel, A. J. Read, C. W. Potter, J. R. Nicolas, A. J. Westgate, D. A. Pabst, Ontogenetic allometry and body composition of harbour porpoises (*Phocoena phocoena*, L.) from the western North Atlantic. *J. Zool.* **257**, 457–471 (2002).

85. D. P. Domning, O. A. Aguilera, Fossil Sirenia of the West Atlantic and Caribbean region. VIII. *Nanosiren garciae*, gen. et sp. nov. and *Nanosiren sanchezi*, sp. nov. *J. Vertebr. Paleontol.* **28**, 479–500 (2008).

86. W. F. Perrin, M. L. L. Dolar, C. M. Chan, S. J. Chivers, Length-weight relationships in the spinner dolphin (*Stenella longirostris*). *Mar. Mamm. Sci.* **21**, 765–778 (2005).

87. S. H. Montgomery, J. H. Geisler, M. R. McGowen, C. Fox, L. Marino, J. Gatesy, The evolutionary history of cetacean brain and body size. *Evolution* **67**, 3339–3353 (2013).

88. H. Shirihai, B. Jarrett, G. M. Kirwan, *Whales, Dolphins, and Other Marine Mammals of the World* (Princeton Univ. Press, 2006).

89. V. Bouetel, C. de Muizon, The anatomy and relationships of *Piscobalaena nana* (Cetacea, Mysticeti), a Cetotheriidae s.s. from the early Pliocene of Peru. *Geodiversitas* **28**, 319–395 (2006).

90. D. K. Sarko, D. P. Domning, L. Marino, R. L. Reep, Estimating body size of fossil sirenians. *Mar. Mamm. Sci.* **26**, 937–959 (2010).

91. P. J. Stacey, R. W. Baird, S. Leatherwood, *Pseudorca crassidens*. *Mar. Mamm. Sci.* **456**, 1–6 (1994).

92. L. P. Folkow, A. S. Blix, Metabolic rates of minke whales (*Balaenoptera acutorostrata*) in cold water. *Acta Physiol. Scand.* **146**, 141–150 (1992).

93. T. A. Jefferson, M. A. Webber, R. L. Pitman, *Marine Mammals of the World: A Comprehensive Guide to Their Identification* (Elsevier, 2008).

94. D. E. Sergeant, P. F. Brodie, Body size in white whales, *Delphinapterus leucas*. *J. Fish. Board Can.* **26**, 2561–2580 (1969).

95. R. W. Baird, R. W. Baird, *Killer Whales of the World: Natural History and Conservation* (Voyageur Press, 2006).

96. S. Agbayani, S. M. E. Fortune, A. W. Trites, Growth and development of North Pacific gray whales (*Eschrichtius robustus*). *J. Mammal.* **101**, 742–754 (2020).

97. S. M. E. Fortune, M. J. Moore, W. L. Perryman, A. W. Trites, Body growth of North Atlantic right whales (*Eubalaena glacialis*) revisited. *Mar. Mamm. Sci.* **37**, 433–447 (2020).

98. R. M. Nowak, *Walker's Mammals of the World* (John Hopkins Univ. Press, 1999).

99. L. Riekkola, V. Andrews-Goff, A. Friedlaender, A. N. Zerbini, R. Constantine, Longer migration not necessarily the costliest strategy for migrating humpback whales. *Aquat. Conserv.* **30**, 937–948 (2020).

100. M. R. McCurry, F. G. Marx, A. R. Evans, T. Park, N. D. Pyenson, S. Kohno, S. Castiglione, E. M. G. Fitzgerald, Brain size evolution in whales and dolphins: New data from fossil mysticetes. *Biol. J. Linn. Soc.* **133**, 990–998 (2021).

101. C. R. McClain, M. A. Balk, M. C. Benfield, T. A. Branch, C. Chen, J. Cosgrove, A. D. Dove, L. C. Gaskins, R. R. Helm, F. G. Hochberg, F. B. Lee, A. Marshall, S. E. McMurray, C. Schanche, S. N. Stone, A. D. Thaler, Sizing ocean giants: Patterns of intraspecific size variation in marine megafauna. *PeerJ* **3**, e715 (2015).